2015 International Nuclear Atlantic Conference - INAC 2015
São Paulo, SP, Brazil, October 4-9, 2015
ASSOCIAÇÃO BRASILEIRA DE ENERGIA NUCLEAR - ABEN
ISBN: **978-85-99141-06-9**

I-125 SEED DOSE ESTIMATES IN HETEROGENEOUS PHANTOM

Isabela S. L. Branco[1], Paula C. G. Antunes[1], Tássio A. Cavalieri[1], Eduardo S. Moura[1] Carlos A. Zeituni[1] and Hélio Yoriyaz[1]

[1] Instituto de Pesquisas Energéticas e Nucleares (IPEN / CNEN - SP)
Av. Professor Lineu Prestes 2242
05508-000 São Paulo, SP
isabela.slbranco@gmail.com

ABSTRACT

Brachytherapy plays an important role in the healing process involving tumors in a variety of diseases. Several studies are currently conducted to examine the heterogeneity effects of different tissues and organs in brachytherapy clinical situations and a great effort has been made to incorporate new methodologies to estimate doses with greater accuracy. The objective of this study is to contribute to the assessment of heterogeneous effects on dose due to I-125 brachytherapy source in the presence of different materials with different densities and chemical compositions. The study was performed in heterogeneous phantoms using materials that simulate human tissues. Among these is quoted: breast, fat, muscle, lungs (exhaled and inhaled) and bones with different densities. Monte Carlo simulations for dose calculation in these phantoms were held and subsequently validated. The model 6711 I-125 seed was considered because it is widely used as a brachytherapy permanent implant and the one used in clinics and hospitals in Brazil. Thermoluminescent dosimeters TLD-700 (LiF: Mg, Ti) were simulated for dose assess. Several tissue configurations and positioning of I-125 sources were studied by simulations for future dose measurements. The methodology of this study so far shall be suitable for accurate dosimetric evaluation for different types of brachytherapy treatments, contributing to brachytherapy planning systems complementation allowing a better assessment of the dose actually delivered to the patient.

1. INTRODUCTION

Radiation therapy can be defined as a treatment which uses ionizing radiation to destroy or control growth of neoplastic cells. The main types of radiation therapy are brachytherapy and teletherapy. In teletherapy, the emission source is positioned externally to the patient and the ionizing radiation beam travels some distance to the tumor, also reaching all structures positioned between its paths. Brachytherapy uses one or more radioactive sealed sources, placed in a short distance to the tumor, where they have contact with the area to be treated preserving the healthy surrounding tissues that should not be irradiated.

In a typical radiotherapy service about 10% to 20% of patients are treated with brachytherapy [1,2]. The dose calculation methodologies and experimental measurements involving brachytherapy sources in general are described with detail in Task Group 43 (TG-43) [3], a document published by the working group of the AAPM (American Association of Physics in Medicine). This protocol defines water as the homogeneous medium where dosimetry is performed. The whole dosimetry is performed considering energy deposition around a single source positioned at the center of a sphere of water. Thus, the influence of heterogeneity tissues and applicators, attenuation between radioactive sources, and the finite patient's dimensions are all ignored leading to the necessary of another solution method with greater accuracy.

The model based dose calculation algorithms (MBDCAs) offer the ability to not limit the dose calculation only in water, allowing the calculation in other medium (tissues, applicators,

air-tissue interfaces). It also takes into account complex geometries models for radiation transport simulations. The MBDCAs allowed heterogeneity corrections to be incorporated into planning systems in radiotherapy. However, in brachytherapy, several studies are currently being conducted to examine the effects of heterogeneity between different tissues and organs in clinical situations and a great effort has been made to incorporate new methodologies to estimate doses with greater accuracy. The recommendations for clinical implementation of this new dosimetric model are described with detail in TG-186 [4].

In view of these methods, the dose deposition study is important, considering the different tissues heterogeneity, and providing more physically accurate models for the exact reconstruction of the dose distribution actually delivered to the patient.

This paper aims to contribute to the studies of heterogeneous effects on brachytherapy dosimetry with ^{125}I source. Monte Carlo simulations were performed to evaluate the dose distribution. Also, a calculation method that uses Burlin cavity theory (MCT -"medium-sized cavity theory") was incorporated for comparison and validation of the simulations results containing different configurations of sources, thermoluminescent dosimeters (TLD-700) and phantoms using tissue equivalent materials.

2. MATERIALS AND METHODS

2.1. MCNP Simulations

MCNP code stands out as one of the most distinguished Monte Carlo based radiation transport codes. The program is suited to simulate interactions of photons, electrons, and neutrons with matter throughout an user-defined problem geometry and material compositions. Its design enables the simulation of wide sort of problems, where the general source definition and geometrical specification is possible [5].

Monte Carlo simulations were performed using the MCNP-4C code [5] for radiation transport. Different tissue configurations and placement of the ^{125}I sources were studied culminating in four simulated arrangements combining, PMMA plates, tissue-equivalent cylinders, thermoluminescent dosimeters and ^{125}I seeds.

Initially represented phantoms were composed entirely of polymethylmethacrylate (PMMA - $\rho = 1.18$ g.cm^3) and then were inserted other heterogeneous materials which simulated human tissue with known densities and compositions. . The heterogeneous materials considered are: bone ($\rho = 1.92$ g.cm^3), adipose tissue ($\rho = 0.95$ g.cm^3), lung tissue ($\rho = 0.26$ g.cm^3) and soft tissue ($\rho = 1.05$ g.cm^3). Figure 1 shows the simulated phantom. In addition to the phantoms, thermoluminescent dosimeters (TLDs) were modeled as detectors, represented by volume cells where energy deposition in calculated. The TLD used were type 700 in the micro cube form with dimensions of 1x1x1 mm^3, sensitive to gamma radiation and consisting almost entirely of lithium fluoride (LiF).

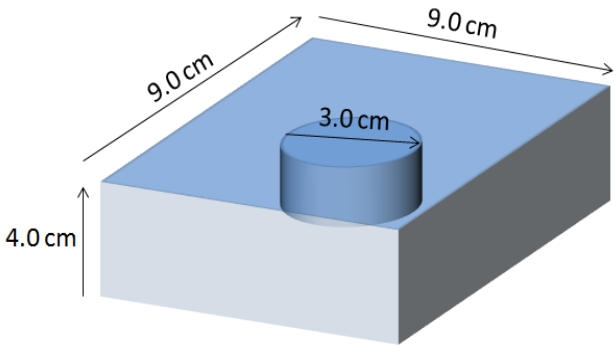

Figure 1: Representation of the model phantom simulated containing an inner cylinder composed by heterogeneous material.

The ionizing radiation sources are ^{125}I seeds. This radioisotope has a half-life of 59.408 days and its decay accompanies photon emissions with an average energy of 29 keV (although represented by an energy distribution in the simulations) having low penetration power. The Amersham ^{125}I model 6711 seed was chosen because it is widely used as a permanent implant in brachytherapy.

In the simulations only photon transport was considered and because the complex geometry of the source, a rejection technique was used, resulting in a 80% sampling efficiency. Figure 2 illustrates the composition and geometry used for ^{125}I seeds description for simulation.

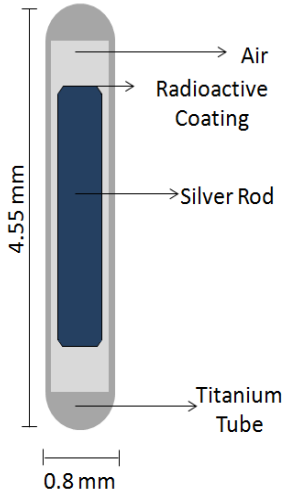

Figure 2: Representation of ^{125}I seed's composition and geometry used in simulations.

Different arrangements using three cited structures (Phantom, TLDs and ^{125}I Seed) are described to understand the four simulated arrangements.

2.2. Simulations

All simulated arrangements consisted of 9 x 9 cm^2 plates with variable thickness and an inner cylindrical hole with 1.5 cm radius where heterogeneous disk materials can be inserted. Five simulations were performed for each of the four phantom configurations using heterogeneous materials. Atomic data related to these materials were obtained from National Institute of Standards and Technology database (NIST) [7].

2.2.1. Simulations 1 and 2

In simulation 1 (Figure 3a) the ^{125}I seed was positioned in the center of the phantom and 42 TLDs (microcubes) distributed around it forming circumferences, with radius of 0.5 cm, 0.75 cm, 1.0 cm, 2.0 cm, 3.0 cm and 4.0 cm, and placed in angle steps of 10^0. Simulation 2 (Figure 3b) adopted similar configuration, differing only in the distance, so the source was positioned at the center and 10 TLDs were distributed with distances of 0.3 cm, 0.5 cm, 0.6 cm, 0.9 cm and 1 cm. In these simulations, the TLDs are in symmetrical positions relative to the source, so that, equivalent results are expected for TLDs placed in the same radius.

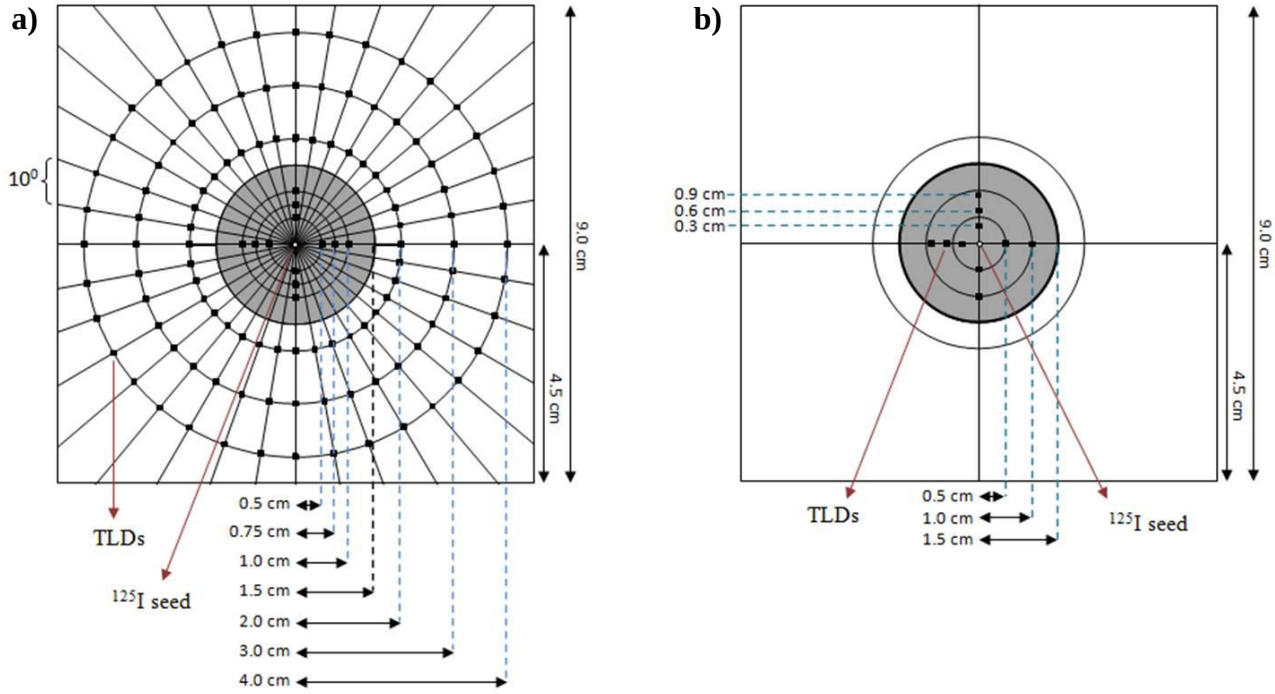

Figure 3: Phantom geometry of simulations 1 (a) and 2 (b) explaining the distances of the ^{125}I source , positioned in the center, and the TLDs-700, with dimension of $1mm^3$ placed around the source (top view).

2.2.2. Simulation 3

In Simulation 3 (Figure 4) a micro cube TLD-700 was placed in the center and the ^{125}I seeds were distributed around it forming a circumference with radius of 0.6 cm, and 1.2 cm and angle step of 60^0.

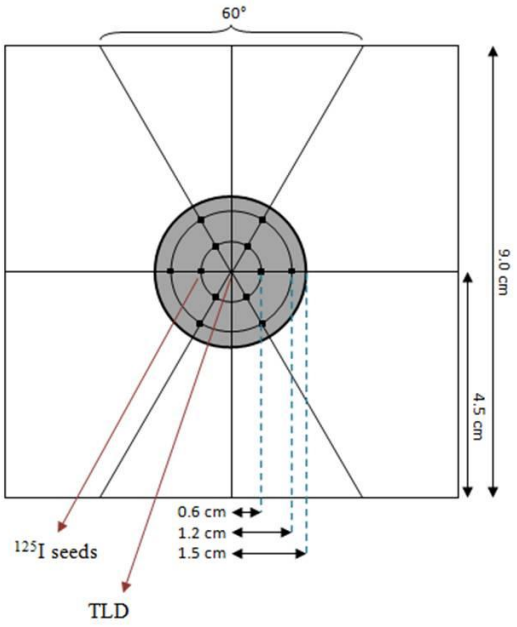

Figure 4: Phantom geometry of simulation 3 showing the distances between the TLD-700, positioned in the center, and the ^{125}I sources (model 6711) surrounding the dosimeter (top view).

The simulation 3 consists of three plates each one with 12 sources and only the central plate contains a TLD. All four plates have thickness of 1.0 cm each as schematized in Figure 5.

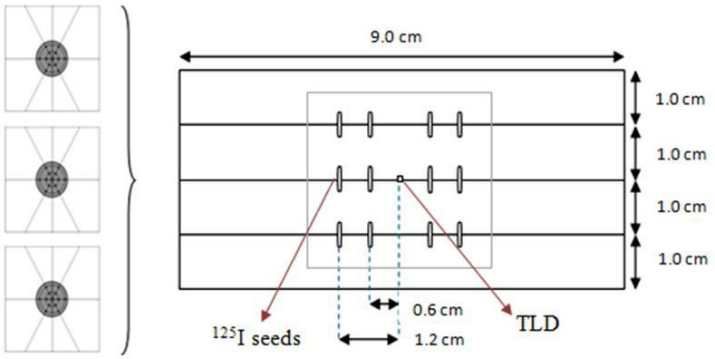

Figure 5: Geometry adopted in the simulation 3. In the picture, the TLD appears in the center of the phantom and the sources are arranged around it. The radial distances were maintained as shown in Figure 4.

In this simulation all the structures were simulated, with influence of the anisotropy of some sources. In total there were 36 simulated ^{125}I seeds, distributed in three layers and only one TLD. The source definitions were similar to the simulations 1 and 2, but 36 cells were used, presenting consequently 36 positions for these cells.

2.2.3. Simulation 4

In simulation 4 (Figure 6) ^{125}I seed was positioned horizontally and only 1 TLD was used in the form of micro cube. The heterogeneous material was inserted in the inner cylindrical hole between the seed and the TLD, distancing them by 0.3 cm. In this simulation, there was also no source anisotropy.

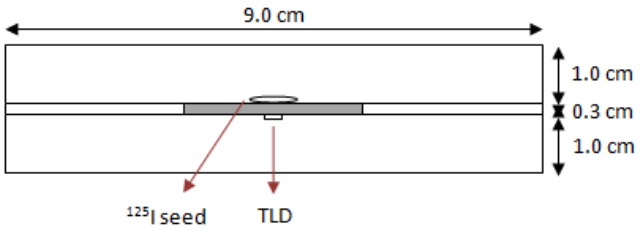

Figure 6: Phantom geometry of simulation 4 explaining the distances between the TLD-700 and the ^{125}I source (model 6711) and the position of heterogeneous material with 0,2 cm (side view).

2.3. Dose Distribution Calculation

Energy deposition was scored using MCNP tally cards in each thermoluminescent dosimeter for each irradiation arrangement. For this purpose we used:

- *F4 - calculates the energy fluence by the particle path length in units of MeV/cm^2
- F6 - calculates the kerma in units of MeV/g.
- *F8 - estimates the energy deposited by electrons and photons in units of MeV.

The tally *F4 was used along with the DE/DF auxiliary cards for dose calculation performed according to the Burlin cavity theory.

2.4. Cavity Theory

To determine the absorbed dose in medium there must be a radiation sensitive instrument present. In general, this instrument differs on their atomic number and density from the medium where they are inserted, representing a discontinuity, which characterizes a cavity in the medium.

W. H. Bragg and L. H. Gray were the first to establish a cavity theory, based on two conditions. The first is that the cavity is small compared to the range of the charged particles generated by the radiation interaction with the cavity; the second condition is that the energy deposited in the cavity is exclusively due to particles passing through it.

Many improvements have been proposed for this theory for situations where the Bragg-Gray conditions are not always fulfilled in practice. Burlin was the first to consider the attenuation of the electrons generated in the medium and the increase of electrons generated in the cavity. The Burlin cavity theory can be applied for small cavities, medium or large; it is given by the equation:

$$\frac{D_{cav}}{D_{med}} = d\left(\frac{S}{\rho}\right)_{med}^{cav} + (1-d)\left(\frac{\mu_{en}}{\rho}\right)_{med}^{cav} \quad (1)$$

The methodology presented by S.B. Scarboro et al. [6] allows to establish following equations for the application of Burlin cavity theory.

$$MCT = d\left(\frac{S}{\rho}\right)_{med}^{cav} + (1-d)\left(\frac{\mu_{en}}{\rho}\right)_{med}^{cav} \quad (2)$$

$$D_{med} = \sum_{E} \psi_E \left(\frac{\mu_{en}}{\rho}\right)_{med,E} \quad (3)$$

$$D_{TLD} = \sum_{E} \left(\psi_E \frac{\mu_{en}}{\rho}_{med,E} \left(MCT_{med}^{TLD}\right)_E \right) \quad (4)$$

And (S/ρ) - collision stopping power; d - a factor that depends on the size of the cavity (in this paper is fixed) and the penetration of the electrons according to energy; (μ_{en} / ρ) - mass energy absorption coefficient; ψ_{en} - energy fluence; D_{cav} - absorbed dose in the cavity and D_{med} - absorbed dose in the medium of interest.

Thus, the energy fluence is calculated by *F4 and the DE/DF auxiliary cards allow interpolation of the table Energy (MeV) by $(\mu_{en} / \rho_{med,E})$ .MCT_E, enabling this calculation is made by the MCNP 4C.

3. RESULTS AND DISCUSSION

Conversions of the obtained tallies results were made to establish comparisons. Thus, the final answers were provided in Gy/s (J/kg.s), assuming the activity of each seed as 0.3 mCi. Values were modified according the response provided by each one of the tallies.

In simulations 1 and 2, the TLDs symmetrical arrangement around the ^{125}I source allows organizing the results according to the radius variation and the type of material used in the inner cylinder. For equal distances, the dose rates results were similar and therefore have been represented as a mean value. Figure 7 shows the obtained dose rates according to these parameters to the tally *F8 considered as a reference (Figure 7a), and the relative differences of tallies *F4 and F6 compared to *F8 (Figures 7c and 7d respectively).

Statistics uncertainties have increased in direct proportion to the distance between the source and the TLD of interest. Comparing the results of the tallies it is observed that the tally *F4 presented, in general, the larger difference values. Figure 2b complements the information of Figure 2a providing the dose rate relative difference from heterogeneous materials in comparison to PMMA, there is large differences mainly in corresponding values of bone tissue and differences of up to about 20% in other materials.

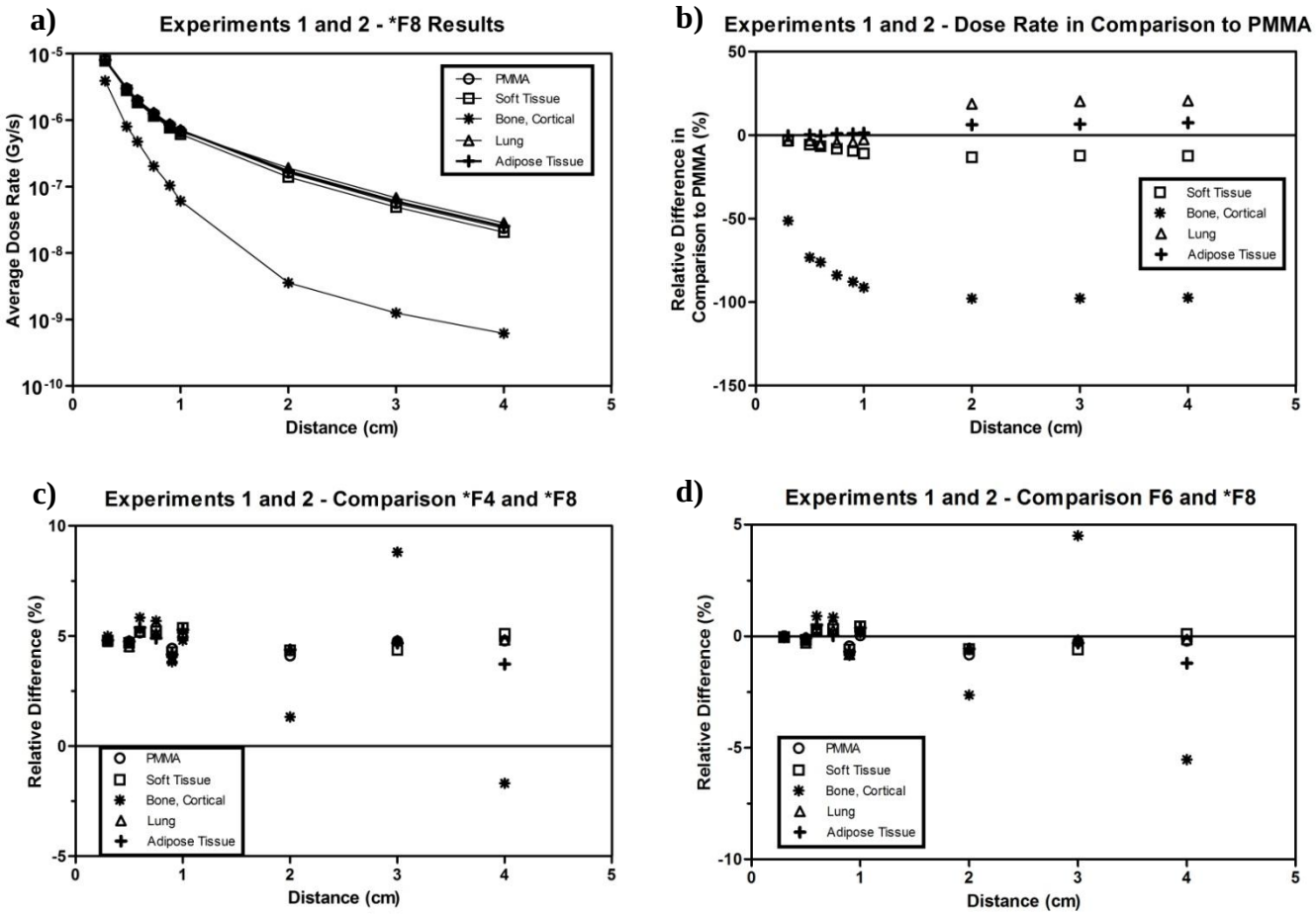

Figure 7: Graphs referring to simulation 1 an 2 relating the distance to dose rates obtained with results F8* regarded as a reference (a), the dose rate relative difference from heterogeneous materials in comparison to PMMA (b), and relative differences of tallies *F4 (c) and F6 (d) compared with *F8.

In simulation 3 the contributions of 36 sources were recorded in the central TLD, resulting in a single value of dose rate for each material used and for each tally as shown in Table 1. This simulation resembles a condition of treatment prostate.

Comparing the results it can be noted that dose values of F6 and *F8 still remain nearby, as well as the large discrepancies in dose rate in bone tissue and PMMA as heterogeneous materials.

Table 1: Tallies results of simulation 3

Inner Cylinder Materials	Dose Rate (Gy/s)	Relative Difference in Comparison to *F8 (%)		Relative Difference in Comparison to PMMA (%)
	*F8	*F4	F6	
PMMA	4.893E-06	4.120	-0.740	-
Soft tissue	4.376E-06	4.289	-0.571	-10.571
Bone, Cortical	6.323E-07	4.153	-0.607	-87.078
Lung	4.740E-06	5.073	0.211	-3.139
Adipose Tissue	4.957E-06	4.359	-0.500	1.294

In Simulation 4, the dose distribution was accounted in one TLD, resulting in a single value of dose rate for each material used and for each tally as shown in Table 2.

Table 2: Tallies results of simulation 4

Inner Cylinder Materials	Dose Rate (Gy/s)	Relative Difference in Comparison to *F8 (%)		Relative Difference in Comparison to PMMA (%)
	*F8	*F4	F6	
PMMA	4.837E-06	4.871	0.031	-
Soft tissue	4.702E-06	4.730	-0.114	-2.782
Bone, Cortical	1.888E-06	4.788	-0.204	-60.973
Lung	5.000E-06	4.751	-0.091	3.375
Adipose Tissue	4.901E-06	4.700	-0.130	1.337

For this simulation, comparisons of results performed in simulation 3 were repeated however there is a decrease in dose rates relative difference comparing PMMA and others heterogeneous materials.

4. CONCLUSIONS

The effects were observed at a dose in accordance with the heterogeneities inserted (representing different human tissues). In the simulations, the dose did not vary significantly with the use of tallies F6 and *F8. One possible explanation for the observed dose variation due to the use of *F4 tally includes the theory of Burlin cavity, since the range of the electrons generated by the source ^{125}I is small (due to low energy) such that the dimensions of TLDs used constitute a large cavity with respect to range of electrons, influencing the dose.

Comparing the different heterogeneous materials there have been significant differences in dose rates values, the main one being observed in bone tissue. These data emphasize the importance of study heterogeneous effects on brachytherapy dosimetry.

This study aims to contribute to ongoing research in brachytherapy medical physics group of the CEN, and the future for a planning model in brachytherapy to provide better evaluation of the dose actually delivered to the patient.

ACKNOWLEDGMENTS

The authors acknowledge CAPES for partially supporting this project.

REFERENCES

1. "Programa de Qualidade em Radioterapia- curso de atualização para técnicos em radioterapia," http://www.inca.gov.br/pqrt/download/tec_int/PQRT_curso_atual_tec_rdtrp_p1.pdf (2013)
2. E. B. Podgorsak, *Radiation oncology Physics: A Handbook for Teachers and Students*, IAEA, Vienna, Austria (2005).
3. M. J. Rivard *et al*, "Update of AAPM Task Group No. 43 Report: A revised AAPM protocol for brachytherapy dose calculations", *Medical Physics*, **31**, pp. 633-674 (2004).
4. L. Beaulieu *et al*, "Report of the Task Group 186 on model-based dose calculation methods in brachytherapy beyond the TG-43 formalism: Current status and recommendations for clinical implementation" *Medical Physics*, 39, pp. 6208-36 (2012).
5. Oak Ridge National Laboratory. *MCNP4C Monte Carlo N-Particle Transport Code System*; RSICC Computer Code Collection, Los Alamos National Laboratory, Los Alamos, New México, (2000)
6. S. B. Scarboro *et al.* "Variations in photon energy spectra of a 6 MV beam and their impact on TLD response", *Medical Physics*, **38**, pp. 2619-2628 (2011).
7. "Physical Measurement Laboratory; National Institute of Standards and Technology", http://physics.nist.gov/PhysRefData/Star/Text/ESTAR-t.html (2015).